ACSNANO
www.acsnano.org
ARTICLE

Piezotronic Effect Enhanced Label-Free Detection of DNA Using a Schottky-Contacted ZnO Nanowire Biosensor

Xiaotao Cao,[†] Xia Cao,*[,†,‡] Huijuan Guo,[†] Tao Li,[†] Yang Jie,[†,‡] Ning Wang,*[,§] and Zhong Lin Wang*[,†,∥]

[†]Beijing Institute of Nanoenergy and Nanosystems, Chinese Academy of Sciences, National Center for Nanoscience and Technology (NCNST), Beijing 100083, P. R. China

[‡]School of Chemistry and Biological Engineering and [§]Center for Green Innovation, School of Mathematics and Physics, University of Science and Technology Beijing, Beijing 100083, China

[∥]School of Material Science and Engineering, Georgia Institute of Technology, Atlanta, Georgia 30332-0245, United States

Supporting Information

ABSTRACT: **A sensitive and *in situ* selective label-free DNA sensor based on a Schottky-contacted ZnO nanowire (NW) device has been developed and utilized to detect the human immunodeficiency virus 1 gene in this work. Piezotronic effect on the performance of the DNA sensor is studied by measuring its output current under different compressive strains and target complementary DNA concentrations. By applying a −0.59% compressive strain to a ZnO NW-based DNA sensor, the relative current response is greatly enhanced by 454%. A theoretical model is proposed to explain the observed behaviors of the DNA sensor. This study provides a piezotronically modified method to effectively improve the overall performance of the Schottky-contacted ZnO NW-based DNA sensor.**

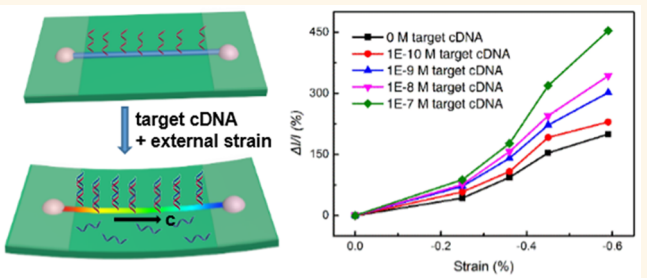

KEYWORDS: *ZnO nanowire, label-free, DNA sensor, piezotronic effect*

Nucleic acid detection has found extensive applications in genotyping, clinical diagnostics, and biomedical research, which has aroused interest in developing sensitive, rapid, and cost-effective detection methods.[1−3] Optical detection and real-time PCR are typical methods for nucleic acids detection; however, these approaches usually require fluorescence-labeled oligonucleotides, optical detectors, and expensive detection processes.[4,5] On the other hand, recent advances in label-free detection of DNA have shown great promise for offering simple, low cost, and sensitive detection of DNA.[6] Because of their high surface to volume ratio, nanomaterials, especially one-dimensional materials, have shown promising performance on label-free detection of DNA.[7,8]

Recently, semiconducting nanowires (NWs) have drawn considerable attention in the fields of electronics, optoelectronics, energy sciences, and sensors.[9−12] By functionalization with chemical or biochemical species at the surface, semiconductor NW-based field effect transistors (FETs) are good candidates for chemical and biological detection.[13,14] Although ohmic contacted FETs are more common for various sensors, detection is largely dependent on the change of conductance of small size nanowires, which makes them difficult to fabricate.[15] Different from ohmic-contacted devices, the performance of the Schottky contacted devices can be tuned by Schottky barrier height (SBH) across the metal−semiconductor (M−S) interface.[16,17] In order to optimize the performance of Schottky contact FETs, effective approaches are needed to tune the SBH.

Wurtzite/zinc blend structured semiconductor materials, such as CdS, CdSe, GaN, and ZnO, have impressive performance on chemical and biochemical molecular identification due to their semiconductive and piezoelectric properties.[18] The piezoelectric potential, which is created by applying an external strain to these one-dimensional materials, can significantly affect their transport properties through increasing or decreasing the SBH. This phenomenon is referred to as the piezotronic effect.[18] The piezopotential existed in the *c*-axis of the nanowire acts as "gate voltage" for tuning and controlling the transport of carriers at the junction/interface.[19] Taking advantage of this piezotronic effect, performance of the NW-based devices can be significantly enhanced by simply applying an external strain.[20,21]

In this work, we present a sensitive and *in situ* selective label-free DNA sensor. This sensor that is also a Schottky contacted

Received: June 22, 2016
Accepted: August 1, 2016

DOI: 10.1021/acsnano.6b04121
ACS Nano XXXX, XXX, XXX−XXX

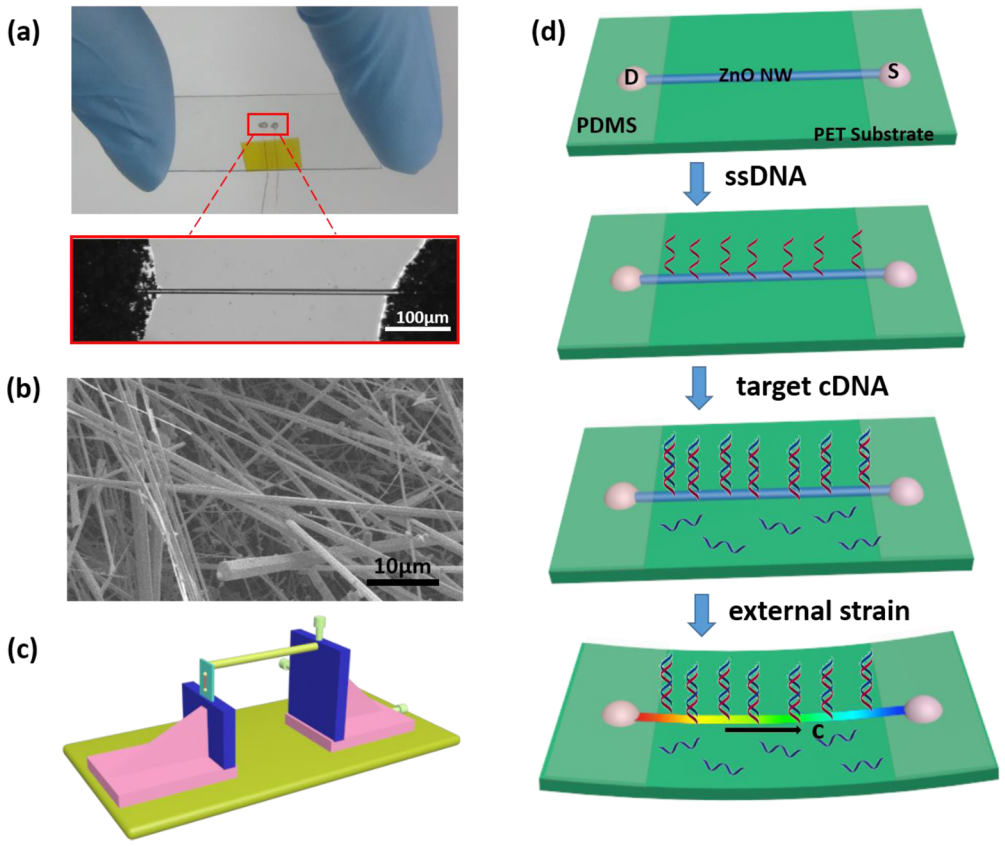

Figure 1. (a) Digital image and optical microscopy image of the ZnO NW DNA sensor. (b) SEM image of the as-synthesized ZnO NWs. (c) Schematic illustration of the experimental setup. (d) Functionalization and detection process of the ZnO NW DNA sensor under no strain and external strain.

ZnO NW FET and can be easily fabricated. The ZnO NW-based FET is highly sensitive to charged species and can be used to increase or decrease the SBH.[22] We utilized this kind of device to detect the human immunodeficiency virus 1 (HIV1) gene.[23] Here, the ZnO NW of the FET device is functionalized with single-stranded DNA (ssDNA) that can selectively hybridize with the target complementary DNA (cDNA). The target cDNA is complementary to the ssDNA. When the negatively charged target cDNA, is hybridized with the ssDNA decorated on ZnO NW, it will be adsorbed on the surface of the ZnO NW. Therefore, the ZnO NW DNA sensor can be used for the selective detection of target cDNA. This selectivity was proved by measuring the output response of DNA sensor to different noncomplementary DNA (non-cDNA) concentrations. Moreover, we demonstrated the piezotronic effect can be used to significantly affect the performance of the DNA sensor by testing its performance under different external strains and target cDNA concentrations. The results show that when applying a −0.59% compressive strain on the ZnO NW based DNA sensor, the relative current response was greatly enhanced by 454%. This study provides a prospective method to effectively improve the overall performance of the Schottky-contacted ZnO NW DNA sensor.

RESULTS AND DISCUSSION

A sensitive and *in situ* selective label-free DNA sensor has been fabricated in our experiment, which is based on a Schottky-contacted ZnO NW device. The real device is presented in Figure 1a, which shows its typical digital image and optical microscopy image. ZnO NWs used in this device were synthesized *via* a vapor−liquid−solid process.[24,25] The synthesized ZnO micro/nanowires were characterized by scanning electron microscopy (SEM), as shown in Figure 1b. The length of the synthesized ZnO micro/nanowires is several hundreds of micrometers, and the diameter varies from tens of nanometers to several micrometers. Figure 1c shows the schematic of the experimental setup. In order to study the piezotronic effect on the performance of this DNA sensor, we fixed one end of the device to the setup and bent the other end through a 3D mechanical stage with the movement resolution of 1 μm, as shown in Figure 1c.

Figure 1d illustrates the functionalization and detection process of the ZnO NW device. In brief, 10 μL of ssDNA solution was dripped onto the surface ZnO NW and kept at 35 °C for 1 h. Then the ssDNA-functionalized device was washed with phosphate-buffered saline (PBS, pH 7.2−7.4) several times to remove the weakly bonded or free-standing ssDNA.[23] The hybridization reaction between the ssDNA functionalized on the surface of ZnO NW and the target cDNA was carried out by adding 10 μL of target cDNA solution on the ZnO NW and kept at room temperature for 1 h. The response of the sensor to different target cDNA concentrations was investigated under different external strains and measured in order to study the piezotronic effect, as shown in Figure 1d.

To demonstrate the successful immobilization of ssDNA on the ZnO NW surface, we carried out the fluorescence emission analysis by using the carboxyfluorescein (FAM)-labeled ssDNA to decorate the ZnO NW instead of the ssDNA. The FAM is a fluorescent dye that exhibits strong fluorescence emission with the excitation wavelength of 494 nm. The ZnO NW shows extremely weak fluorescence under the 494 nm excitation laser,

DOI: 10.1021/acsnano.6b04121
ACS Nano XXXX, XXX, XXX−XXX

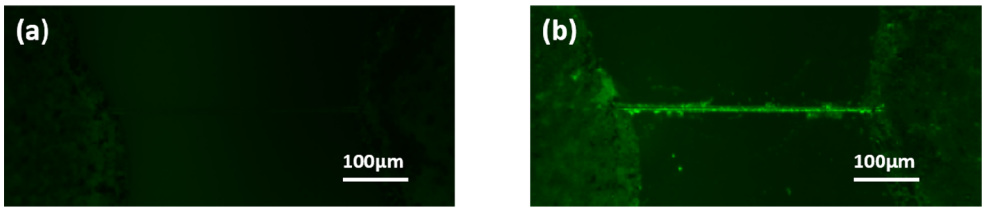

Figure 2. Fluorescence microscopy images of (a) ZnO NW and (b) ZnO NW functionalized with FAM-labeled ssDNA with the excitation wavelength of 494 nm.

as shown in Figure 2a. However, after we functionalized the ZnO NW with FAM-labeled ssDNA, the functionalized ZnO exhibited strong fluorescence and the surface of the ZnO NW became rough, as shown in Figure 2b. This result indicates that the ssDNA has been successfully immobilized onto the surface of the ZnO NW.

In order to investigate the performance of the DNA sensor, we systematically measured its output currents under different target cDNA concentrations and compressive strains. Figure 3 shows five sets of $I-V$ curves and a 3D graph that were measured at different conditions. The five sets of $I-V$ curves measured at the bias voltage ranging from −1.5 to +1.5 V present the nonsymmetrical and nonlinear character, which indicates the different Schottky barrier heights at the two contacts. The two Schottky barriers at the M−S interfaces, which are critical to the electrical transport property of this device, behave like two back-to-back connected diodes.[21,26] Under positive or negative bias voltage, the transport property is mainly controlled by the reversely biased Schottky barrier.

Parts a and b of Figure 3 show the performance of the DNA sensor under 0.00 and −0.59% compressive strain, respectively, with the target cDNA concentration ranging from 0 to 1×10^{-7} M. The output current of this device was significantly increased at both 0.00 and −0.59% compressive strain conditions when the concentration of target cDNA was reduced. As shown in Figure 3a, under 0.00% strain, the output current increased from 0.26 to 0.89 μA (by 242%) when the target cDNA concentration decreased from 1×10^{-7} to 1×10^{-10} M. Figure 3b shows the output current increased from 1.44 to 2.94 μA (by 104%) under −0.59% compressive strain with the same target cDNA concentration change. Under 0.00% strain, the output current difference between 1×10^{-7} and 1×10^{-10} M target cDNA concentration was 0.63 μA. The output current difference was 1.50 μA as the compressive strain increased to −0.59%, increasing by 138%. These results indicated the DNA sensor exhibited a higher response at a lower DNA concentration, and the difference between two target cDNA concentrations was largely improved by the piezotronic effect.

Parts c and d of Figure 3 illustrate the piezotronic effect on the performance of the DNA sensor in detail, in which $I-V$ curves are tested at the target cDNA concentration of 1×10^{-10} and 1×10^{-7} M, respectively. These two $I-V$ curves show that the output current significantly increased as the compressive strain was gradually raised. At the fixed concentration of 1×10^{-10} M, the output current increased from 0.89 to 2.94 μA (by 230%) when the compressive strain increased from 0.00 to −0.59%, as presented in Figure 3c. With the same compressive strain change, the current increased from 0.26 to 1.44 μA (by 454%) at a fixed concentration of 1×10^{-7} M, as shown in Figure 3d. From these results, we can see that the piezotronic effect greatly enhanced the performance of the ZnO NW DNA sensor. The $I-V$ curves under other compressive strains and target cDNA concentrations exhibit similar trends (Figure S1).

The selectivity of the DNA sensor to target cDNA was demonstrated by comparing the output currents measured at different non-cDNA and target cDNA concentrations. The non-cDNA does not match the ssDNA immobilized on the surface of the ZnO NW. Figure 3e presents the $I-V$ curves of the DNA sensor which were measured at the 0.00% strain with the non-cDNA concentration ranging from 0 to 1×10^{-7} M. With the decrease of non-cDNA concentration, the output current increased only a small amount. The current increased from 0.76 to 1.02 μA (by 34.2%) when the concentration of non-cDNA was reduced from 1×10^{-7} and 1×10^{-10} M. This output current change in Figure 3e is obviously smaller than that illustrated in Figure 3a, which increased by 242%. When different compressive strains were applied to this device, the output currents increased on the whole but the difference between two non-cDNA concentrations is still small. Thus, the DNA sensor is not sensitive to the non-cDNA solution even with different applied compressive strains (Figure S2), demonstrating good selectivity to the target cDNA.

In order to clearly present the overall performance of this device at different target cDNA concentrations and compressive strains, all of the results were organized and plotted in a 3D graph, as shown in Figure 3f. From the 3D graph, we can easily see an overall trend that the output currents at a bias voltage of 1.5 V largely increase with the increase of compressive strains or the decrease of target cDNA concentrations. More details and information on these results are given in Figure 4a−d by four 2D graphs.

Parts a and b of Figure 4 show the absolute and relative current responses, which were measured at the bias voltage of 1.5 V, to different external compressive strains at a fixed target cDNA concentration of 0, 1×10^{-10}, 1×10^{-9}, 1×10^{-8}, and 1×10^{-7} M, respectively. Figure 4a illustrates five curves that present a similar trend where the output current obviously increases with the increase of externally applied compressive strain. For example, at a fixed target cDNA concentration of 1×10^{-9} M, the current increased from 0.58 to 2.33 μA as the external strain ranged from 0.00 to −0.59%, increasing by 302%. It should be noted that the output current of the DNA sensor was 1.14 μA under the target cDNA concentration of 0 M and 0.00% strain. Under the target cDNA concentration of 1×10^{-7} M and −0.59% compressive strain, the output current became 1.44 μA, which demonstrated the piezotronic effect had a greater effect on the performance of the DNA sensor than the target cDNA concentration. Figure 4b shows the relative current response increased with the increase of externally applied compressive strain. Under the target cDNA concentration of 1×10^{-7} M and −0.59% compressive strain, the relative current response was up to 454%. These results indicate the device gives higher resolution at a larger external strain for the presence of piezotronic effect.

DOI: 10.1021/acsnano.6b04121
ACS Nano XXXX, XXX, XXX−XXX

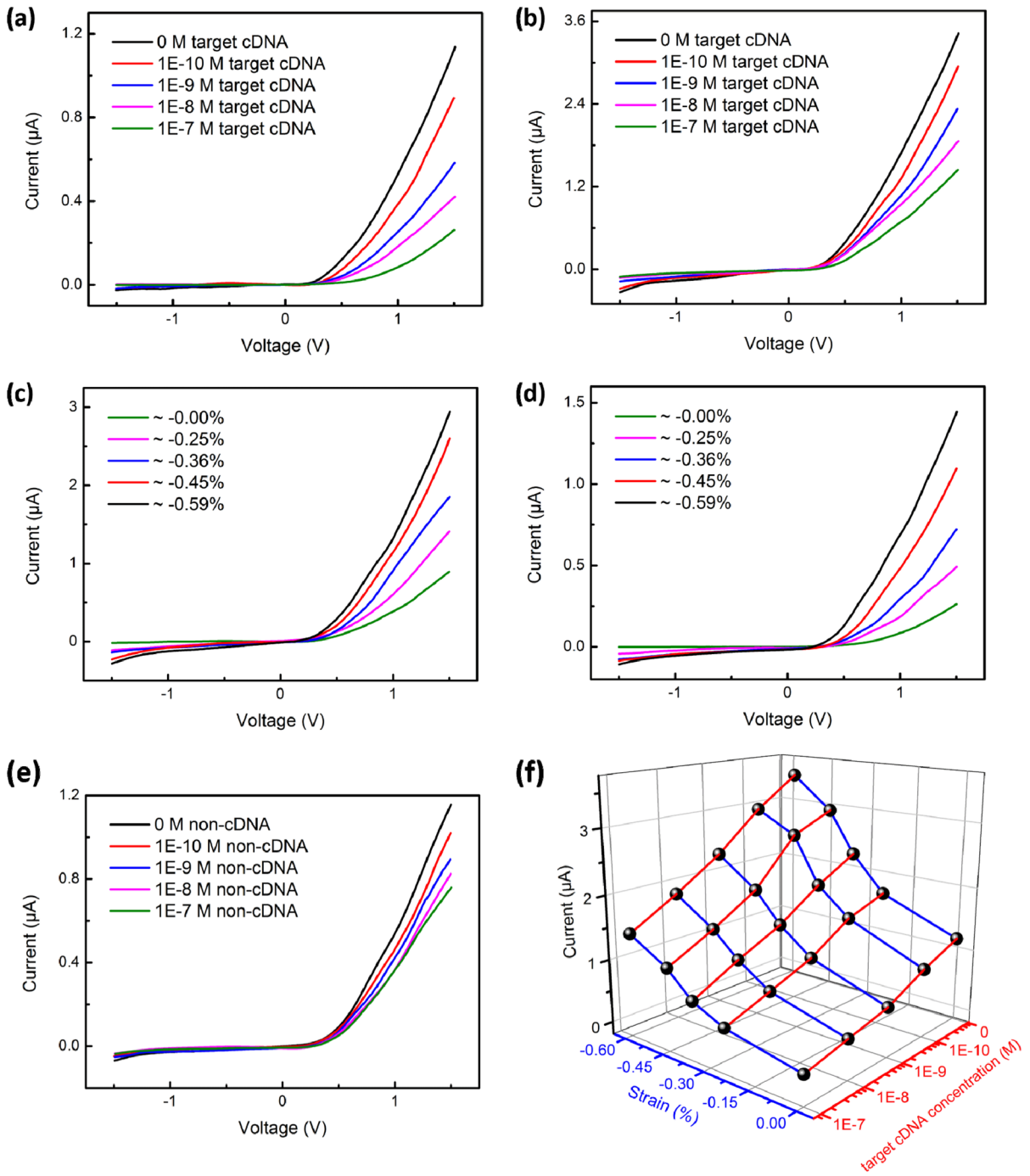

Figure 3. ***I*–*V*** **curves of the DNA sensor under different compressive strains and DNA concentrations with a bias voltage from −1.5 to 1.5 V under (a) 0.00% strain, (b) −0.59% compressive strain with the target cDNA concentration ranging from 0 to 1×10^{-7} M and under target cDNA concentrations of (c) 1×10^{-10} M and (d) 1×10^{-7} M with different compressive strains ranging from 0 to −0.59%. (e)** ***I*–*V*** **curves of the DNA sensor under 0.00% strain with the non-cDNA concentration from 0 M to 1×10^{-7} M. (f) Current response of the DNA sensor to different compressive strains and target cDNA concentrations under a bias voltage of 1.5 V.**

Parts c and d of Figure 4 present the absolute and relative current responses to different target cDNA concentrations under fixed external strain of 0.00, −0.25, −0.36, −0.45, and −0.59%, respectively. It can be seen from each curve in Figure 4c that the output current raises with the decrease of target cDNA concentration. The output current increased with the decrease of target cDNA concentration, which indicated the ZnO NW DNA sensor gave higher output current at a lower target cDNA concentration. Figure 4d shows the device exhibited higher relative current response at a lower DNA concentration, which indicated this device may be suitable for the relatively low concentration detection of DNA. Furthermore, from the point of external strain, the output current increased when we applied an increasing external compressive strain to this DNA sensor. As a whole, the performance of the ZnO NW DNA sensor under different target cDNA concentrations is significantly enhanced by the piezotronic effect.

DOI: 10.1021/acsnano.6b04121
ACS Nano XXXX, XXX, XXX−XXX

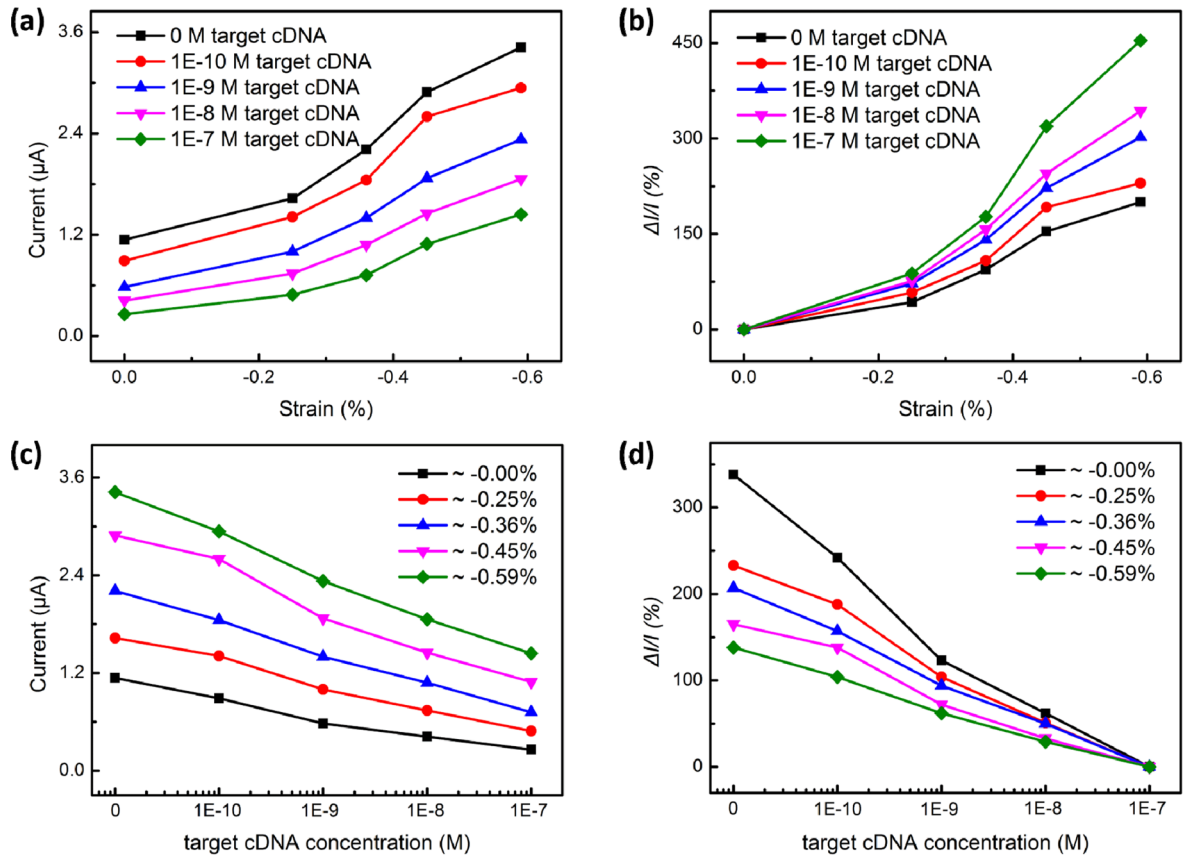

Figure 4. Enhanced performance of the ZnO NW DNA sensor by the piezotronic effect. (a, b) Absolute and relative current response of the DNA sensor to compressive strain at a fixed target cDNA concentration of 0, 1×10^{-10}, 1×10^{-9}, 1×10^{-8}, snf 1×10^{-7} M, respectively. (c, d) Absolute and relative current response of the DNA sensor to target cDNA concentration at a fixed compressive strain of 0.00, −0.25, −0.36, −0.45, and −0.59, respectively.

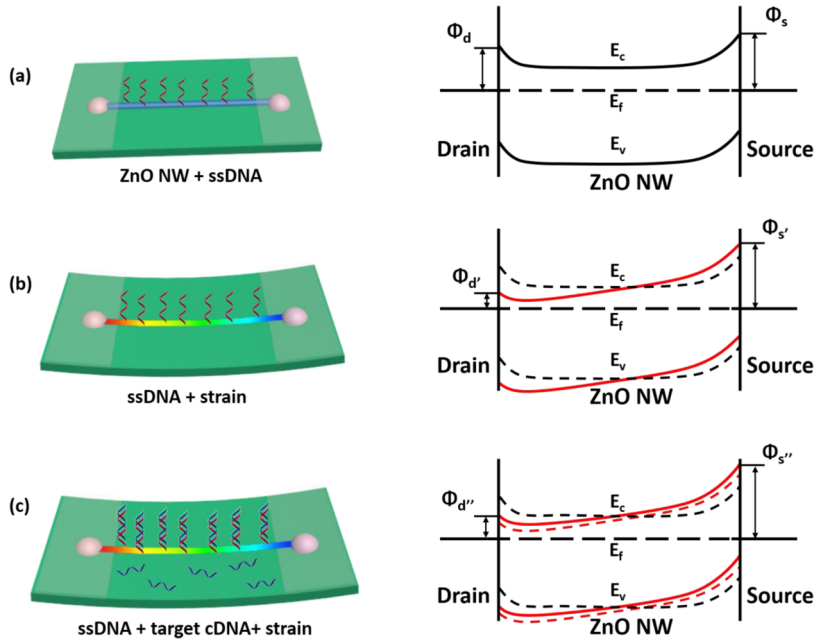

Figure 5. Schematic band diagrams of the ZnO NW DNA sensor under different conditions: (a) unstrained, (b) compressively strained and functionalized with ssDNA but without the target DNA, (c) compressively strained, functionalized with ssDNA, and hybridized with the target DNA.

In order to explain the enhanced performance of this DNA sensor by the piezotronic effect, a theoretical model is proposed using energy band diagrams, as presented in Figure 5. The energy band structure of the unstrained ZnO NW DNA sensor is given

DOI: 10.1021/acsnano.6b04121
ACS Nano XXXX, XXX, XXX−XXX

in Figure 5a. Two silver electrodes and the ZnO NW form a metal−semiconductor−metal (M−S−M) structure and the Schottky barrier at one M−S contact is different from the other. The transport property of this device is dominantly controlled only by the reversely biased Schottky barrier, and here, it is the Schottky barrier at the drain electrode, Φd.

Figure 5b shows the energy-band change of the DNA sensor under compressive strain. When a compressive strain was applied to the DNA sensor, a piezopotential was created inside the ZnO NW along the *c*-axis. In this condition, the piezopotential at the drain electrode was positive, which reduced the height of Schottky barrier; the piezopotential at the other side (source electrode) was negative, which increased the SBH. Because the Φ_d played a dominant role in controlling the transport property of this device, the decrease of SBH at the drain electrode would lead to an increase in the output current of the device. Moreover, the larger the applied compressive strain within certain range, the higher the output current and sensitivity of the DNA sensor. Therefore, we can utilize the change of compressive strain to effectively tune the transport property of the DNA sensor.

The target cDNA, which is negatively charged, is complementary to the ssDNA and can selectively hybridize with the ssDNA immobilized on the ZnO NW. When we introduced the target cDNA solution with certain concentration to this DNA sensor, the target cDNA was absorbed on the surface of the functionalized ZnO NW and hybridized with ssDNA. Compared with the compressive-strained DNA sensor without target cDNA, the absorption and hybridization of negatively charged target cDNA to this device resulted in a depletion of the electron carriers and increased all the Schottky barriers of drain and source electrodes, as shown in Figure 5c. The increase in Φ_d gave rise to the decrease in output current of this device. When we increased the concentration of target cDNA, the output current lowered more. It should be noted that the effect of target cDNA to this device is much weaker than the strain-induced piezotronic effect. That is to say, though the absorption and hybridization of target DNA increased the Schottky barrier of the drain electrode, the applied compressive strain decreased it much more. As a whole, the Schottky barrier of the drain electrode was reduced by the combination effect of target cDNA and piezotronic effect, as illustrated in Figure 5c. Therefore, the output current of this compressive-strained DNA sensor with target cDNA still increased much, compared with the unstrained DNA sensor without target cDNA. This theoretical model explains the change of output current with the variation of compressive strain and target cDNA concentration, and also explains the enhanced performance of the ZnO NW DNA sensor.

CONCLUSIONS

In summary, a Schottky-contacted ZnO NW device was presented for the sensitive and *in situ* selective label-free detection of DNA. The performance of the ZnO NW DNA sensor was investigated by measuring its output currents under different external strains and target cDNA concentrations. By applying different compressive strains, the performance of this device was significantly enhanced for the presence of piezotronic effect. The results demonstrate that both the output currents and the difference between two target cDNA concentrations are largely improved by utilizing the piezotronic effect. The energy band diagrams of the DNA sensor is illustrated to explain the results observed in this work. This study provides a piezotronic-assisted method for the label-free detection of DNA with high sensitivity and selectivity.

METHODS

Reagents. Lyophilized oligonucleotides were synthesized and purified by the Sangon Biotech Co., Ltd. The sequence of HIV1 gene is 5′-AGTCAGTGTGGAAAATCTCTAGC-3′, which is the target cDNA. The sequence of ssDNA is 5′-GCTAGAGATTTTCCACACT-GACT-3′, which is complementary to the target cDNA. The sequence of the FAM-labeled ssDNA is the same as ssDNA, which is 5′-GCTAGAGATTTTCCACACTGACT-FAM-3′. The sequence of non-cDNA is 5′-CGCCCTCTTCTTGTGGATG-3′. The PBS (0.01M, pH 7.2−7.4) was purchased from Beijing Solarbio Science & Technology Co., Ltd. All other chemicals used in this study were G.R. grade and purchased from Alfa Aesar.

ZnO Micro/Nanowire Synthesis. ZnO micro/nanowires used in this study were prepared through a vapor−liquid−solid growth process.[24,25] ZnO nanopowder (1 g) and activated carbon powder (1 g) were mixed uniformly. Then the mixture was transferred to an alumina boat, which was placed at the center of the tube furnace, with a silicon substrate horizontally put on its top. This silicon substrate was coated with a 5 nm gold layer, and the gold layer faced down. The temperature of the furnace tube was kept at 960 °C for 1 h with the carrier gas flow rate of 60 sccm argon and 20 sccm oxygen. The product was collected after the reaction was completed.

DNA Sensor Fabrication. The DNA sensor was fabricated by transferring an individual ZnO NW onto a polyethylene terephthalate substrate. Then the two end well.[20] After that, two silver electrodes were fully covered by a layer of epoxy to avoid the possible contact between the electrodes and DNA solution during the following tests. A 10 μL portion of ssDNA solution with certain concentration was dripped onto the surface of ZnO NW and maintained at 35 °C for 1 h in a small airtight container. Then the ssDNA-functionalized device was washed with PBS several times to remove the weakly bonded or free-stood ssDNA.[23] The ssDNA-functionalized DNA sensor was ready for use.

ASSOCIATED CONTENT

Supporting Information

The Supporting Information is available free of charge on the ACS Publications website at DOI: 10.1021/acsnano.6b04121.

Additional information and figures (PDF)

AUTHOR INFORMATION

Corresponding Authors

*E-mail: caoxia@ustb.edu.cn.
*E-mail: wangning@buaa.edu.cn.
*E-mail: zlwang@gatech.edu.

Notes

The authors declare no competing financial interest.

ACKNOWLEDGMENTS

This research was supported by the National Natural Science Foundation of China (NSFC Nos. 21575009, 21173017, 51272011, and 21275102), the Program for New Century Excellent Talents in University (NCET-12-0610), the Science and Technology Research Projects from Education Ministry (213002A), the National "Twelfth Five-Year" Plan for Science & Technology Support (No. 2013BAK12B06), and the "Thousands Talents" Program for a Pioneer Researcher and His Innovation Team, China, National Natural Science Foundation of China (Grant No. 51432005; No. Y4YR011001).

REFERENCES

(1) Hutvágner, G.; McLachlan, J.; Pasquinelli, A. E.; Bálint, É.; Tuschl, T.; Zamore, P. D. A Cellular Function for the RNA-Interference Enzyme Dicer in the Maturation of the Let-7 Small Temporal RNA. *Science* **2001**, *293*, 834−838.

DOI: 10.1021/acsnano.6b04121
ACS Nano XXXX, XXX, XXX−XXX

(2) Lee, J. K.; Jung, Y. H.; Stoltenberg, R. M.; Tok, J. B. H.; Bao, Z. Synthesis of DNA-Organic Molecule-DNA Triblock Oligomers Using the Amide Coupling Reaction and Their Enzymatic Amplification. *J. Am. Chem. Soc.* **2008**, *130*, 12854−12855.
(3) Heller, M. J. DNA Microarray Technology: Devices, Systems, and Applications. *Annu. Rev. Biomed. Eng.* **2002**, *4*, 129−153.
(4) Ho, H. A.; Najari, A.; Leclerc, M. Optical Detection of DNA and Proteins with Cationic Polythiophenes. *Acc. Chem. Res.* **2008**, *41*, 168−178.
(5) Giulietti, A.; Overbergh, L.; Valckx, D.; Decallonne, B.; Bouillon, R.; Mathieu, C. An Overview of Real-Time Quantitative PCR: Applications to Quantify Cytokine Gene Expression. *Methods* **2001**, *25*, 386−401.
(6) Drummond, T. G.; Hill, M. G.; Barton, J. K. Electrochemical DNA Sensors. *Nat. Biotechnol.* **2003**, *21*, 1192−1199.
(7) Hahm, J.; Lieber, C. M. Direct Ultrasensitive Electrical Detection of DNA and DNA Sequence Variations Using Nanowire Nanosensors. *Nano Lett.* **2004**, *4*, 51−54.
(8) Li, Z.; Chen, Y.; Li, X.; Kamins, T.; Nauka, K.; Williams, R. S. Sequence-Specific Label-Free DNA Sensors Based on Silicon Nanowires. *Nano Lett.* **2004**, *4*, 245−247.
(9) Pan, C.; Luo, Z.; Xu, C.; Luo, J.; Liang, R.; Zhu, G.; Wu, W.; Guo, W.; Yan, X.; Xu, J. Wafer-Scale High-Throughput Ordered Arrays of Si and Coaxial Si/Si1−x Ge x Wires: Fabrication, Characterization, and Photovoltaic Application. *ACS Nano* **2011**, *5*, 6629−6636.
(10) Cui, Y.; Lieber, C. M. Functional Nanoscale Electronic Devices Assembled Using Silicon Nanowire Building Blocks. *Science* **2001**, *291*, 851−853.
(11) Wang, Z. L.; Song, J. Piezoelectric Nanogenerators Based on Zinc Oxide Nanowire Arrays. *Science* **2006**, *312*, 242−246.
(12) Patolsky, F.; Zheng, G.; Lieber, C. M. Nanowire-Based Biosensors. *Anal. Chem.* **2006**, *78*, 4260−4269.
(13) Duan, X.; Li, Y.; Rajan, N. K.; Routenberg, D. A.; Modis, Y.; Reed, M. A. Quantification of the Affinities and Kinetics of Protein Interactions Using Silicon Nanowire Biosensors. *Nat. Nanotechnol.* **2012**, *7*, 401−407.
(14) Zheng, G.; Patolsky, F.; Cui, Y.; Wang, W. U.; Lieber, C. M. Multiplexed Electrical Detection of Cancer Markers with Nanowire Sensor Arrays. *Nat. Biotechnol.* **2005**, *23*, 1294−1301.
(15) Kuang, Q.; Lao, C.; Wang, Z. L.; Xie, Z.; Zheng, L. High-Sensitivity Humidity Sensor Based on a Single SnO_2 Nanowire. *J. Am. Chem. Soc.* **2007**, *129*, 6070−6071.
(16) Yu, R.; Pan, C.; Chen, J.; Zhu, G.; Wang, Z. L. Enhanced Performance of a ZnO Nanowire-Based Self-Powered Glucose Sensor by Piezotronic Effect. *Adv. Funct. Mater.* **2013**, *23*, 5868−5874.
(17) Wang, N.; Gao, C.; Xue, F.; Han, Y.; Li, T.; Cao, X.; Zhang, X.; Zhang, Y.; Wang, Z. L. Piezotronic-Effect Enhanced Drug Metabolism and Sensing on a Single ZnO Nanowire Surface with the Presence of Human Cytochrome P450. *ACS Nano* **2015**, *9*, 3159−3168.
(18) Wang, Z. L. Piezopotential Gated Nanowire Devices: Piezotronics and Piezo-Phototronics. *Nano Today* **2010**, *5*, 540−552.
(19) Wang, Z. L. Preface to the Special Section on Piezotronics. *Adv. Mater.* **2012**, *24*, 4630−4631.
(20) Yu, R.; Pan, C.; Wang, Z. L. High Performance of ZnO Nanowire Protein Sensors Enhanced by the Piezotronic Effect. *Energy Environ. Sci.* **2013**, *6*, 494−499.
(21) Niu, S.; Hu, Y.; Wen, X.; Zhou, Y.; Zhang, F.; Lin, L.; Wang, S.; Wang, Z. L. Enhanced Performance of Flexible ZnO Nanowire Based Room-Temperature Oxygen Sensors by Piezotronic Effect. *Adv. Mater.* **2013**, *25*, 3701−3706.
(22) Yeh, P. H.; Li, Z.; Wang, Z. L. Schottky-Gated Probe-Free ZnO Nanowire Biosensor. *Adv. Mater.* **2009**, *21*, 4975−4978.
(23) Li, B.; Pan, G.; Avent, N. D.; Lowry, R. B.; Madgett, T. E.; Waines, P. L. Graphene Electrode Modified with Electrochemically Reduced Graphene Oxide for Label-Free DNA Detection. *Biosens. Bioelectron.* **2015**, *72*, 313−319.
(24) Pan, Z. W.; Dai, Z. R.; Wang, Z. L. Nanobelts of Semiconducting Oxides. *Science* **2001**, *291*, 1947−1949.
(25) Zhu, G.; Zhou, Y.; Wang, S.; Yang, R.; Ding, Y.; Wang, X.; Bando, Y.; Wang, Z. Synthesis of Vertically Aligned Ultra-Long ZnO Nanowires on Heterogeneous Substrates with Catalyst at the Root. *Nanotechnology* **2012**, *23*, 055604.
(26) Xue, F.; Zhang, L.; Feng, X.; Hu, G.; Fan, F. R.; Wen, X.; Zheng, L.; Wang, Z. L. Influence of External Electric Field on Piezotronic Effect in ZnO Nanowires. *Nano Res.* **2015**, *8*, 2390−2399.

DOI: 10.1021/acsnano.6b04121
ACS Nano XXXX, XXX, XXX−XXX